NUMERICAL SIMULATION OF OXY-FUEL AND CO-FIRING PROCESS OF COAL AND BIOMASS IN AN ACTUAL STEAM GENERATOR

Cristiano Vitorino da Silva, cristiano@uricer.edu.br
Pedro Lando Bellani, pedrolandobellani@gmail.com
Department of Mechanical Engineering – Universidade Regional Integrada do Alto Uruguai e das Missões – URI, Erechim, RS, Brazil.

Fernando Marcelo Pereira, fernando@mecanica.ufrgs.br
Department of Mechanical Engineering – Federal University of Rio Grande do Sul - UFRGS, Porto Alegre, RS, Brazil.

Maria Luiza Sperb Indrusiak, mlsperb@unisinos.br
Graduate Program in Mechanical Engineering – University of Vale do Rio dos Sinos – UNISINOS, São Leopoldo, RS, Brazil.

Paulo Smith Schneider, pss@mecanica.ufrgs.br
Department of Mechanical Engineering – Federal University of Rio Grande do Sul - UFRGS, Porto Alegre, RS, Brazil.

Abstract. *This paper performs a numerical study in CFD about the oxy-fuel process of a mixture of coal with woody biomass in an actual steam generator of approximately 320 MW in a co-firing process. The aim of this study is to verify the feasibility of this steam generator to work with this combustion process which is going to be a global trend, since its application can reduce the environmental impact due to emissions, going to meet the increasingly demanding legal issues. A numerical model, based on the technique of finite volumes was implemented in ANSYS CFX software for the solution of differential equations of conservation of mass, momentum, energy and chemical species and turbulence and radiation models. Different study cases involving co-firing and oxy-fuel process were analyzed to compare with the actual operation conditions of the equipment, which burns pulverized coal, verifying the possibility of implementing this new alternative to burning also biomass. Results showed that oxy-fuel combustion processes, and co-firing, when evaluated in separate processes, presented pollutant reductions, such as NOx, CO and CH_4. However, the addition of biomass also reduces the flame temperature, in comparison with the actual burning process using just coal as a fuel. Combining the two methods, a significant reduction in pollutants was achieved, keeping almost the same levels of temperature inside the furnace, however with a significant decrease in the average heat flux on the walls.*

Keywords*: Pulverized Coal, Biomass, CFD, Co-firing, Oxy-fuel.*

1. INTRODUCTION

Combustion as a means of heat generation has been used since the discovery of fire. According Warnatz et al. (1999), in the last decades about 90% of all electricity generated worldwide was coming from a combustion process. According to the World Coal Association, if maintained the current demand for fossil fuels, coal reserves will have a lifespan of about 112 years, while the oil and natural gas reserves 46 and 54 years respectively. These data together with the concern in reducing the production of greenhouse gases, justify the wide interest in research in combustion processes in power plants.

The great global goal is to generate more energy, emitting less pollutant and extending the life of fossil fuels. Combining the burning of these fossil fuels to renewable fuels, such as wood biomass from forestry, it can extend further coal reserves and minimize environmental impacts. Associating also more efficient processes, such as oxy-fuel, an even longer life can be achieved for these reserves. The oxy-fuel process could be combined to CCS (Carbon Capture and Storage) cycles, contributing to minimization of CO_2 emissions. Many are the authors that investigate the oxy-fuel process (Croiset and Thambimuthu, 2001; Liu *et al.*, 2005; Bhuiyan and Naser, 2014; Bhuiyan and Naser, 2015) all indicated this technique as an efficient form to burn non-renewable fuels. In another line, co-firing process can prolong the life time of fossil fuels and collaborate for a reduction of global greenhouse gases, as presented by some important works such as Sami *et al.* (2001), Williams et al. (2001), Yin et al. (2010), Gubba et al. (2012) and Silva et al. (2014).

This work presents a numerical study of the oxy-fuel process of a mixture of coal with woody biomass in a steam generator of approximately 320 MW. A numerical model based on finite volume technique was implemented in ANSYS CFX software for the solution of differential equations of mass conservation, momentum, energy and chemical species balances, along with turbulence and radiation models. Different case studies were analyzed involving co-firing and oxy-fuel process in order to compare these combustion techniques with the actual operating condition of the equipment, that burns only pulverized coal, verifying the possibility of implementation of those new alternative techniques.

2. MATHEMATICAL FORMULATION

2.1 Mathematical formulation for coal combustion

The kinetic scheme for coal particles pyrolysis used in this work was proposed by Silva et al. (2010), assuming that coal is composed of raw coal, ash and moisture. The raw coal decomposes into volatile gases, here CO and CH_4, and residual carbon by two devolatization concurrent reactions, according to Ubayakar et al. (1976). The methane and CO

oxidation are modeled by two overall steps, the WD2 of Westbrok and Drier (1981). Figure 1 shows diagrammatically the mechanisms of coal devolatização and carbon and volatile substances oxidation.

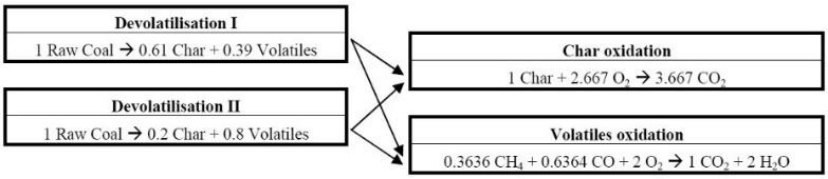

Figure 1. Basic scheme of coal reactions (Ubhayakar,1977).

NOx formation is modeled through the NO-thermal, NO-prompt and NO-fuel mechanisms, according to the simplifications proposed by the methodology implemented in ANSYS - CFX (Ansys, 2011). Complementing this formulation, the drying of coal particles model proposed by Xianchun et al. (2009) was used. The kinetic parameters used in this reaction, namely the pre-exponential factor and the activation energy, are respectively 4.587×10^{12} s^{-1} and 78.995 kJ/kmol (Xianchun et al., 2009). For the residual char combustion, the Field Char Oxidation model (Ansys, 2011) was adopted.

2.2 Mathematical formulation for biomass combustion

The kinetic scheme for the pyrolysis of biomass particles used in this work was proposed by Haseli et al. (2011) and assumes that the biomass is composed of raw biomass, ash and water. The raw biomass decomposes into light gases, tar (or heavy gases) and residual carbon through three parallel reactions. The model proposed by Bryden et al. (2002) for drying of wood biomass particles has been implemented. The chemical reaction rates are determined by Arrhenius model, accordingly to Ansys (2011). The kinetic constants were adopted from Di Blasi et al. (2001), accordingly to studies by Haseli et al. (2011), since they have good results for reactor at temperatures above 1100 K. Kinetic constants for particles drying were the same as used by Bryden et al. (2002). According to Grieco et al. (2011), the mass fraction of light gases, tar and residual carbon generated from the raw biomass decomposition are, respectively, 17%, 62% and 21%.

2.2.1 Homogeneous Reactions

The volatile components released during the pyrolysis process may react with other components and oxygen on the core and periphery of the particle. The mass fractions of the produced light gases depend on the heating conditions and the type of biomass. However, for engineering applications a constant composition is generally assumed. Di Blasi et al. (2001) propose the light gas composition to be 0.521, 0.156, 0.271, 0.021 and 0.031 for H_2O, CO, CO_2, CH_4 and H_2 respectively. For tar, an empirical simplification as $C_xH_yO_z$ is used. Bryden et al. (2003) analyzed the decomposition of tar and found that its main products are CO, CO_2, H_2O, H_2, CH_4, C_2H_6, C_2H_4, C_2H_2 and C_3H_6. They propose a chemical formulation represented by $C_{3.878}\ H_{6.426}\ O_{3.561}$, which has an O/C ratio of 0.918 and an H/C ratio of 1.657. Further information to describe the combustion rates of methane, hydrogen, carbon monoxide and tar can be obtained in Haseli et al. (2011). Gasification and combustion of the residual carbon are heterogeneous reactions. The residual carbon gasification rates can also be obtained in Haseli et al. (2011). Gasification and combustion rate for residual carbon are determined through the Field Char Oxidation model adopted for char, incorporating the Arrhenius constants proposed by Hobbs et al. (1992).

2.3 Mass and species conservation

The first equation solved is the mass and species conservation. Assuming a multicomponent fluid, the equation is solved for velocity, pressure, temperature and other quantities of the fluid. The influence of the multiple components is felt only through property variation by virtue of differing properties for the various components. Each component has its own equation for conservation of mass. After Favre-averaging, the species conservation equation can be expressed, in tensor notation, as:

$$\frac{\partial(\bar{\rho}\widetilde{U_j}\widetilde{Y_i})}{\partial x_j} = \frac{\partial}{\partial x_j}\left(\left(\rho D_i + \frac{\mu_t}{Sc_t}\right)\frac{\partial \widetilde{Y_i}}{\partial x_j}\right) + \overline{S_i} \tag{1}$$

where $\widetilde{U_j} = \sum\left(\tilde{\rho}_i \widetilde{U}_{ij}\right)/\bar{\rho}$ is the mass-averaged velocity field [m/s], $\widetilde{\rho_i}$ is the specific mass [kg/m³]; the $\overline{U_j}$ term represents the velocity vector and $\widetilde{U}_{ij}$ is the *ij* component's mass-averaged velocity. The relative mass flux is given by $\rho_i\left(\widetilde{U}_{ij} - \widetilde{U}_j\right)$. The mass fraction of *i* component is defined as $\widetilde{Y_i} = \tilde{\rho}_i/\bar{\rho}$, and the sum of all components' mass fractions is equal to one.

2.4 Momentum conservation

The second equation to solve is the momentum conservation of the fluid, which is given by:

$$\frac{\partial(\bar{\rho}\widetilde{U_i}\widetilde{U_j})}{\partial x_j} = -\frac{\partial p^*}{\partial x_j}\delta_{ij} + \frac{\partial\left(\mu_{eff}\frac{\partial \widetilde{U_i}}{\partial x_j}\right)}{\partial x_j} + \frac{\partial \widetilde{U}}{\partial x_i \partial x_j} + \overline{S_U} \tag{2}$$

where $\mu_{eff} = \mu + \mu_t$; the term μ is the mixture dynamic viscosity and μ_t is the turbulent viscosity, defined as $\mu_t = C_\mu \rho k^2/\varepsilon$. The term p^* is the modified pressure, C_μ is an empirical constant of the turbulence model, which is equal to 0.09. The variable $\bar{\rho}$ is the time-averaged pressure of the gaseous mixture, and δ_{ij} is the Krönecker's delta function; $\overline{S_U}$ is the source term. The Boussinesq model was used to represent the buoyancy force due to density variations, and the *k-ω* model was adopted to provide the turbulence on the flow (Wilcox, 1988).

2.5 Energy conservation

Considering the transport of energy due to diffusion of each chemical species, the energy equation is the third one that needs to be solved. This equation can be written as:

$$\frac{\partial\left(\bar{\rho}\widetilde{U_j}\widetilde{h}\right)}{\partial x_j} = \frac{\partial}{\partial x_j}\left(k_{con}\frac{\partial \tilde{T}}{\partial x_j} + \sum_i^{Nc}\widetilde{h_i}\left(\rho D_i + \frac{\mu_t}{Sc_t}\right)\frac{\partial \tilde{Y}_i}{\partial x_j} + C_p\frac{\mu_t}{Pr_t}\frac{\partial \tilde{T}}{\partial x_j}\right) + \bar{S}_{rad} + \bar{S}_{rea} + \bar{S}_T \quad (3)$$

where $\tilde{T}$, $\tilde{h}$ and C_p are the average temperature, enthalpy and specific heat of the mixture. The term $\tilde{Y}_i$ is the averaged mass fraction of the *i*-th chemical species, k_{con} is the thermal conductivity of the mixture, Pr_t is the turbulent Prandtl number; $\bar{S}_{rad}$, $\bar{S}_{rea}$ and $\bar{S}_T$ represent the sources of thermal energy due to the radiative transfer, the chemical reactions and energy sink. The term $\bar{S}_{rea}$ can be written as:

$$\bar{S}_{rea} = \sum_\alpha \left[\frac{h_i^0}{\overline{MM_i}} + \int_{\tilde{T}_{ref,i}}^{\tilde{T}} C_{p.i}\, d\tilde{T}\right]\overline{R_i} \quad (4)$$

where h_i^0 and $\tilde{T}_{ref,i}$ are the formation enthalpy and the reference temperature of the *i*-th chemical species. To complete the model, the density of the mixture can be obtained from the ideal gas state equation (Kuo, 2005; Turns, 2000), $\bar{\rho} = p\overline{MM}\left(\bar{\Re}\tilde{T}\right)^{-1}$, where p is the combustion chamber operational pressure, which is here set equal to 1 atm, and $\overline{MM}$ is the mixture molecular mass. The mentioned equations are valid only in the turbulent core, where $\mu_t \gg \mu$. Close to the wall, the conventional logarithmic law of the wall is used (Nikuradse, 1933).

2.6 Radiative transfer equation

The radiation intensity can be expressed as:

$$\frac{dI_v(r,s)}{dS} = -(K_{av} + K_{sv}).I_v(\boldsymbol{r},\boldsymbol{s}) + K_{av}I_b(v,T) + \frac{K_{SV}}{4\pi}\int_{4\pi} dI_V(\boldsymbol{r},\boldsymbol{s}')\Phi(\boldsymbol{s}.\boldsymbol{s}')d\Omega' + \dot{S} \quad (5)$$

where v is the frequency, and r and s are the position and direction vectors, respectively. The S term represents the radiation path; K_{av} is the media absortion coefficient, and K_{sv} is the scattering coefficient. The black body emission is given by I_b, and I_v represents the spectral radiation intensity. The solid angle and the phase-function for the scattering is given by Ω and Φ, respectively. There is also a source term, written as $\dot{S}$. In this work it was adopted an isotropic scattering, since pulverized coal generates high levels of particles.

Among several methods to solve radiative equations, it was employed the Discrete Transfer Radiation Model (DTRM) (Carvalho et al., 1991). According to Filkoski (2010), this method presents coherent results and demands a relatively low computational effort, despite its limitations. This work uses the DTRM model with 16 rays. Generally, as a starting point to arrive at a tractable method for calculating radiative properties, the particles were assumed as spherical and homogeneous. In this work, the heat transfer, from gas mixture to particle, considers that the particles are opaque bodies with emissivity equal to one (black bodies), and the Hanz-Marshall correlation was used to model the heat transfer coupling between the gas mixture flow and the particles (Ansys, 2011).

2.6.1 WSGG - weighted-sum-of-gray-gases

The effect of the non-gray gaseous mixture was considered by original WSGG model proposed by Hottel and Sarofim (1967), which compares experimental data with equations, using the following correlation:

$$\varepsilon(pS) = \sum_{i=0}^{N_G} a_j(T)\left(1 - e^{-K_j pS}\right) \quad (6)$$

In the Eq. (6), K_j represents the absorption coefficient, a_j is the weighting coefficient of the j-th gray gas. The gray gases numbers are defined as N_G; K_j is the absorption coefficient of the *j*-th gas. The WSGG model allows us to write the absorption coefficients in the polynomial form, as follows:

$$a_j(T) = \sum_{k=0}^{k} b_{j,k}T^{k-1} \quad (7)$$

Several researchers proposed coefficients for the WSGG model in the last years. Dorigon et al. (2013) proposed new coefficients, adjusting the emittance curves by the LBL – Line-by-Line Integration method, using the HITEMP 2010 database (Rothman et al., 2010). The authors used 4 gray gases, and the coefficients proposed are shown in Tab.1:

2.7 The E-A (Eddy Break Up – Arrhenius) chemical reactions model

The reduced chemical reactions model employed in this work assumes finite rate reactions and a steady state turbulent process to volatiles combustion. In addition, it was considered that the combined pre-mixed and non-premixed oxidation occurs in two global chemical reaction steps, and involving only ten species: O_2, CH_4, H_2, H_2O, *Tar* ($C_{3.878}H_{6.426}O_{3.561}$), HCN, HCO, NOx, CO_2 e CO. Thus, one has the conservation equation for the *i*-th chemical species, given by Eq. (2), where the source term, S_i, considers the average volumetric rate of formation or destruction of the *i*-th chemical species in all chemical reactions. This term is computed from the summation of the volumetric rates of formation or destruction in all the k-th reaction where the *i*-th species is present, $\overline{R_{i,k}}$. Thus, $\overline{R_i} = \sum_k \overline{R_{i,k}}$. A combined Arrhenius-Magnussen model, the EBU-Arrhenius (Eaton et al., 1999), was used to obtain this rate.

Table 1. Coefficients for WSGG model (Dorigon et al., 2013).

j	$K_{g,j}$, [$m^{-1}atm^{-1}$]	$b_{g,j,1}$ x 10^1	$b_{g,j,2}$ x 10^1 [K^{-1}]	$b_{g,j,3}$ x 10^7 [K^{-2}]	$b_{g,j,4}$ x 10^{11} [K^{-3}]	$b_{g,j,5}$ x 10^{14} [K^{-4}]
1	0,192	0,5617	7,8440	-8,5630	4,2460	-7,4400
2	1,719	1,4260	1,7950	-0,1077	-0,6972	1,7740
3	11,370	1,3620	2,5740	-3,7110	1,5750	-2,2670
4	111,016	1,2220	-0,2327	-0,7492	0,4275	-0,6608

3. MODEL VALIDATION

For verification purposes, the combustion model developed in the present work was applied to the study case presented by Gu et al. (2010) which consists in a numerical and experimental study of burning coal process in a simple geometry of a tuyere (injector and burner of coal-oxidizer used in industrial furnaces), a device used to inject and burn coal in steel furnaces, as shown in Fig. 2. The injection lance is inserted in an axial and concentric form to the center of the product line. The inner diameter of the nozzle is 19 mm. The length of the studied tuyere is 580 mm, having a diameter gradual reduction from 166 mm (at the inlet) to 150 mm at 240 mm from the initiation of the tuyere. Comparing the results of Fig. 2a and 2-b, and 2c and 2-d, it can be observed that the two cases show similar velocity and temperature fields. The same modeling developed in this study was also applied to the case shown by Silva et al. (2010), obtaining similar results.

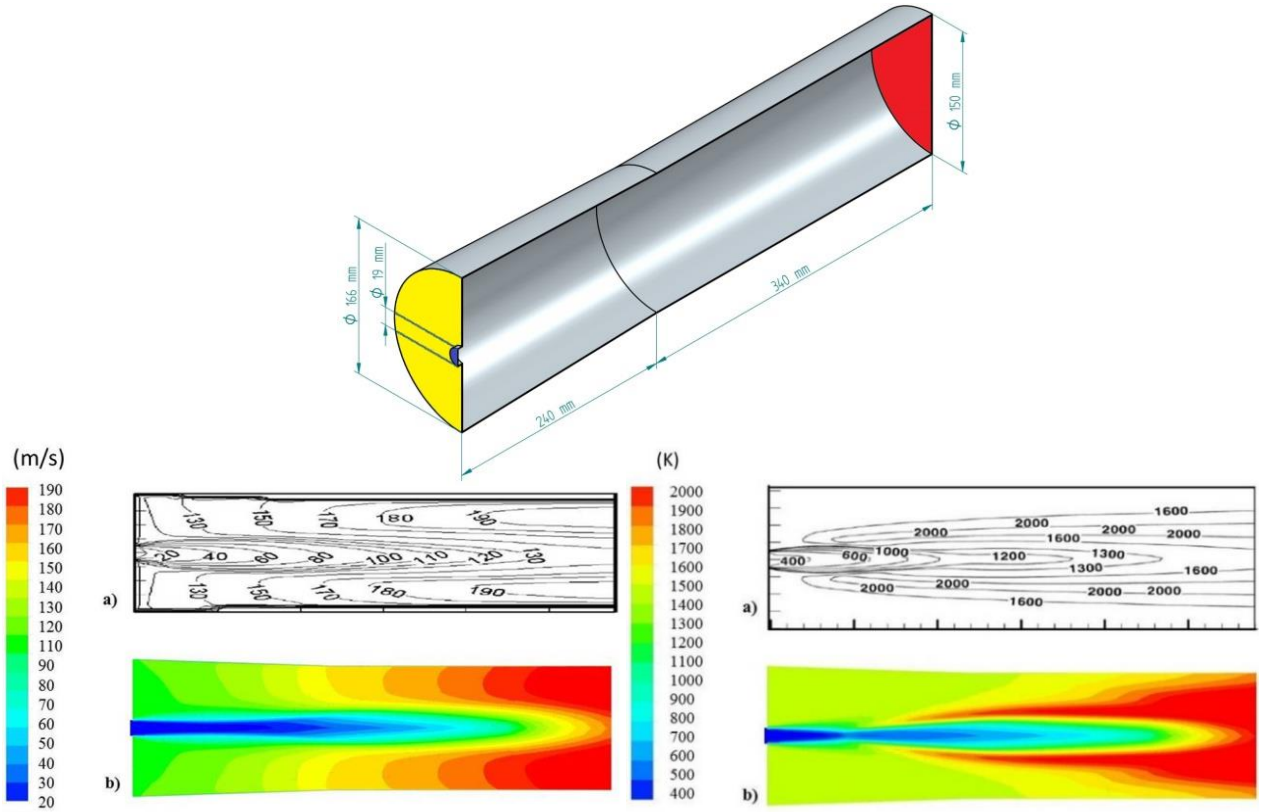

Figure 2 - Temperature and velocity fields obtained from this modeling (b, d) and the results of Gu et al. (2010) (a, c).

4. PHYSICAL MODEL

The boiler in question is part of a 160 MW thermal power plant that uses pulverized coal. The combustion chamber has a square cross section of approximately 11 m and a height of approximately 53 m. The boiler operates through four tangential firing burners located on each corner of the combustion chamber with an inclination of 15° to the horizontal direction. Fig. 3 (c-d) shows the general arrangement of the burner and the horizontal boiler cross section.

Boundary conditions and boiler design data were obtained from Silva et al. (2010), which evaluated the combustion of pure coal. The walls of the boiler, covered with steel tubes, were modeled as crude steel with a fixed temperature of 673 K, this being due to the saturation temperature of the water at the boiler working pressure. Thermal emissivity of the walls was assumed to be 0.9. Air flow, coal and biomass entering the combustion chamber by the burners were set as entry conditions: the mass flow rate of primary and secondary combustion air is 77.57 kg/s and 98.72 kg/s, respectively; pulverized coal and biomass mass flow rates are 47.50 kg/s and 0.84 kg/s, respectively. These values were obtained from Silva et al. (2010) via mass and energy balances (fuel and combustion air) on the boiler, considering a reduction of approximately 5% on coal flow for the inclusion of biomass, considering the actual case, keeping the same thermal load provided for the boiler, about 320 MW. The lower heating value (LHV) of coal and biomass used is 10301 kJ/kg and 14267 kJ/kg, respectively. The temperature of the primary air and coal with biomass is 542 K; the temperature of the secondary air is 600 K. Pulverized coal particles size was modeled by probabilistic Rosin-Rammler distribution (Brown, 1995) and limited between 50 and 200 μm. Biomass particles are consider spherical with 75 μm. Coal type CE 3100 and biomass of wood were used. The proximate and ultimate analysis of coal and wood in dry and wet basis are in Tab. 2.

Table 2. Chemical composition of coal CE 3100 and wood biomass.

	Coal CE 3100 concentration (%) (Silva et al., 2010) LHV = 10301 kJ/kg		**Wood biomass concentration (%) (Mehrabian et al., 2012)** LHV = 14267 kJ/kg	
Proximate Analysis	**DRY BASES**	**WET BASES**	**DRY BASES**	**WET BASES**
Moisture	0	16.47	0	6,00
Volatiles	12.01	26.50	51.40	54.31
Char	33.21	27.74	48.10	45.21
Ash	54.78	45.76	0.50	0.48
Ultimate Analysis				
Oxigen	7.92	6.62	45.53	42.80
Carbon	33.21	27.74	48.10	45.21
Hydrogen	2.34	1.95	5.77	5.42
Sulfur	1.14	0.95	-	-
Nitrogen	0.61	0.51	0.10	0.09

A pressure of -400 Pa was prescribed at the outlet of the modeled domain, based on the operating data. The heat exchangers were modeled as porous media to absorb a certain amount of energy per unit volume. The amounts relating to the energy absorbed in W/m^3 are: ECO2, 62000; LTR, 139000; HTR, 40000; LTS, 98000 and HTS, 88000. In order to evaluate the influence of the particle size on biomass co-firing, six case studies were considered and compared with a case of pure coal burning (base case) on the same operating conditions presented in Silva et al. (2010), although taking into account a model for drying the coal particles. The cases considered respectively the following the simulations are presented in Tab. 3.

Table 3. Analyzed cases.

CASES	**OXIDIZER**	**FUEL**
1A	Air	100% coal
2A	25% O_2 e 75% CO_2	100% coal
3A	30% O_2 e 70% CO_2	100% coal
1B	air	95% coal e 5% wood biomass
2B	25% O_2 e 75% CO_2	95% coal e 5% wood biomass
3B	30% O_2 e 70% CO_2	95% coal e 5% wood biomass

5. GRID COMPUTING

The discretization within the boiler is performed with the implementation of tetrahedral volumes and prismatic volumes near the chamber walls. Figures 2-c and 2-d shows the geometry and the generated mesh in front view and in perspective.

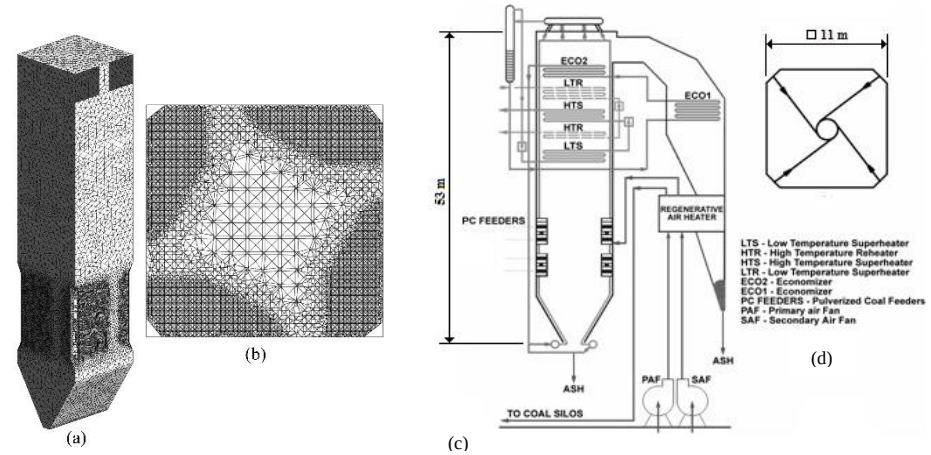

Figure 3. Mesh used in modeling: (a) perspective view and (b) cross section view (Silva et al., 2010); and geometry: (c) general arrangement of the boiler components and (d) horizontal boiler cross section (Silva et al., 2010).

Grid independency tests were carried out among five grid systems with 1.44 million, 2.12 million, 2.70 million and 3.19 million of control volumes. The mesh selected has around 3.19 million elements of different sizes, using mesh refinement in the reactive regions near the burners in a function of computational costs.

6. NUMERICAL METHOD AND MESH INDEPENDENCE TEST

Property fields in the boiler (speed, temperature, pressure, concentration, etc.) were numerically determined using the commercial software Ansys CFX v.15, which is based on the finite volume method (Patankar, 1980). The power law was selected to assess the flow on control's volume surface and the function up-wind was prescribed for the interpolation scheme. The pressure-velocity coupling was solved by the SIMPLE algorithm (Patankar, 1980). As the conservation equations are nonlinear, relaxation factors were used for all conservation equations and additional models.

The mesh designed has about $3.1x10^6$ elements of different sizes, and the density function was used in the regions near to the burners. In order to prove the mesh independence, tests were made to determine the best relation between refinement and computational effort.

7. RESULTS AND DISCUSSION

Figure 4-a shows the field of temperatures of the first three cases studied (1A, 2A and 3A). The cases 2A and 3A show the use of oxy-fuel concentrations of 25% and 30 of O_2, respectively, in the flue gas recirculation. It is possible to realize the expected behavior for the use of oxy-fuel, i.e., an increase in temperature, since the CO_2 has a stronger thermal effect than N_2, because its specific heat is larger. As seen in the literature, the use of oxy-fuel provides an increase in the boiler temperature, which can be seen primarily in the flame region. The insertion of CO_2 as an oxidant complement prevents excessive increase of temperature in the steam generator output, diluting the energy produced in the flame, causing the same role of nitrogen. Figure 5 graphically represents the temperature on a line in the center of the steam generator for cases 1A, 2A and 3A.

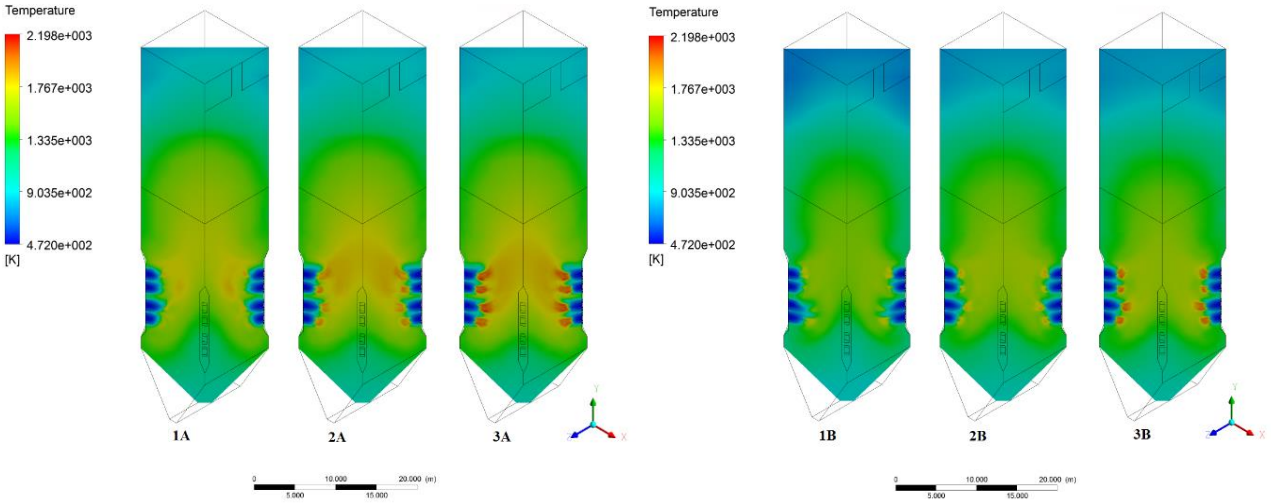

(a) (b)

Figure 4. Temperature fields in a vertical transverse plane in the combustion chamber: (a) cases 1A, 2A e 3A; (b) cases 1B, 2B e 3B.

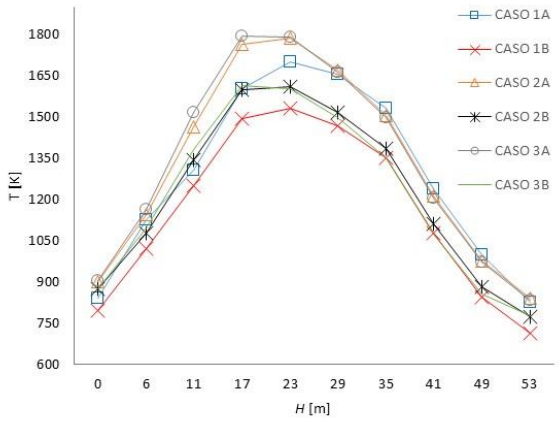

Figure 5. Temperature profiles in relation to boiler height in the axial symmetry line for all cases.

Through Figures 4-a and 5 it is possible to clearly see the influence of oxy-fuel process, which tends to increase the temperature in the combustion zone (11 to 23 m). The influence of O_2 concentration in the oxidizer is also evident. The higher the proportion of O_2 used, the higher the temperature in the burning region. Analyzing the Figure 4 is possible to sense temperature variations in all cases. The use of oxy-fuel, for both cases, as in cases without co-firing has the same trend, increasing the temperature in the combustion region. Through Figure 5 there is a clear temperature drop promoted by the addition of biomass combustion.

The average data in the steam generator output are shown in Tab. 4. Analyzing the Tab. 4 there is a clear reduction of gaseous pollutants such as CO, NOx and CH_4, with the addition of O_2 and CO_2 as oxidizing agents. The fractions of CO and CH_4 dropped 66.44% and 68.75%, respectively for cases 1A, 2A and 3A. As both are incomplete burning of indicators it is clear that the use of oxy-fuel, and reduce the level of greenhouse gases, promoted a more complete burn in the steam generator. Note that methane is effective three to four times more harmful than carbon dioxide to the greenhouse effect, and any reduction of this pollutant will have environmental advantages. Analyzing the data of Tab. 4 for co-firing process, cases B, is also evident the reduction of gaseous pollutants, particularly NOx and CO, with the use of oxy-fuel (2B and 3B). The CO fraction decreased 44.52%, showing that the oxy-fuel showed better efficiency compared to the case of combustion with atmospheric air applied to the coal and biomass mixture.

Table 4. The average data in the steam generator output for all cases.

DATA/CASES	1A	2A	3A	1B	2B	3B
NOx [ppm]	3.28	0.78	1.15	3.35	1.53	1.15
O_2[%]	2.24	3.19	7.12	2.76	3.84	7.89
CO_2 [%]	21.95	87.36	83.29	21.29	87.10	82.87
CO [ppm]	1.46	0.54	0,49	1.46	0.87	0.81
CH_4 [ppm]	0.16	0.06	0.05	0.06	0.06	0.05
Average wall heat flux, q'' [kW/m^2]	138.69	149.04	160.19	115.03	107.41	111.36
Temperature [K]	896.81	897.24	891.03	747.42	814.78	808.18

The three cases referred to by the letter B (1B, 2B and 3B) relate to simulations with the substitution of 5% carbon for 1.74% biomass, with the exception of the case 1B that refer to the use of oxy-fuel in the proportions of 25% O_2 (2B) and 30% O_2 (3B) in the flue gas recirculation. The temperatures fields of cases involving co-firing are shown in Fig. 4-b. Analyzing the Figure 4-b one realizes the same behavior shown in Fig. 4-a, however at lower temperatures. This is due to the use of co-firing, which promotes a decrease in the flame temperature. Although the heating value of biomass is greater than coal, its burning kinetics are not. From the results of the three cases using co-firing it was possible to assemble the Tab. 4, showing the concentration of various data in the output of combustion gases.

Looking at the data, it follows that the addition of biomass in the combustion promotes increased in NOx and reduction of CH_4, but causes a significant temperature drop. However, with the incorporation of oxy-fuel, it has compensation this loss, and to decrease the concentrations of all pollutants in the outlet region of the steam generator.

The use of the two methods together promotes a considerable reduction in polluting gases in 68.75% for CH_4, 44.52% for CO and 64.94% for NOx, when compared with cases 1A and 3B, which represent the cases of current operation of the steam generator and the case of oxy an co-firing process. Analyzing the cases 1A and 3B it was observed a decrease in the average wall heat flux of 138.69 kW/m^2 for 111.36 kW/m^2. On the other hand, this drop causes a decrease in quantity of steam generated and consequently a decrease in the production of generated steam.

8. CONCLUSIONS

Through analysis of the results, it was clear that the proposed model attended the expectations enabling the analysis of the burning process inside the steam generator. The influence of the use of oxy-combustion and co-firing processes concurrently followed the same trend in terms of quality of the results found in the literature (Bhuiyan and Naser, 2015). The two methodologies presented promote significant reductions in pollutant emissions and also provide a reduction in the amount of fossil fuel used as part of the fuel is replaced by woody biomass, which is characterized by being a renewable fuel with zero net CO_2 emissions.

The process of co-firing under the conditions studied in this work, if used alone will display a decrease of approximately 16.67% in the magnitude of temperature of combustion gases in the steam generator output region compared to the original boiler operation. The 3B case that demonstrates the combined use of oxy and co-firing processes presents a temperature decrease of 9.88%, being more appropriate, needing lower levels of operation adjustments for implementation.

9. ACKNOWLEDGEMENTS

The authors thank to CNPq for giving support by granting an IC scholarship to the second author and for the research financial support.

10. REFERENCES

Ansys, 2011. User's guide - CFX Solver Theory.

Asotani, T., Yamashita, T., Tominaga, H., Uesugi, Y., Itaya, Y. and Mori, S., 2008. "Prediction of ignition behavior in a tangentially fired pulverized coal boiler using CFD". *Fuel*, Vol. 87, pp. 482-490.

Bhuiyan, A.A. and Naser, J., 2014. "Computational modelling of co-firing of biomass with coal under oxy-fuel condition in a small scale furnace". *Fuel*., Vol.143, pp. 455-466.

Bhuiyan, A.A. and Naser, J., 2015. " CFD modelling of co-firing of biomass with coal under oxy-fuel combustion in a large scale power plant". *Fuel*., Vol.159, pp. 150-168.

Brown, W. K., 1995. "Derivation of the Weibull distribution based on physical principles and its connection to the Rosin-Rammler and lognormal distributions". *Journal of Applied Physics*, vol. 78, pp. 2758-2763.

Bryden, K. M., Ragland, K. W. and Rutland, C. J., 2002. "Modeling thermally thick pyrolysis of wood". *Biomass and Bioenergy*, vol. 22, pp. 41-53.

Carvalho, M.G., Farias, T. and Fontes, P., 1991. "Predicting radiative heat transfer in absorbing, emitting, and scattering media using the discrete transfer method", *ASME HTD*, Vol. 160, pp.17-26.

Crnomarkovic, N., Sijercic, M., Belosevic, S., Tucakovic, D. and Zivanovic, T., 2013. "Numerical investigation of processes in the lignite-fired furnace when simple gray gas and weighted sum of gray gases models are used". *IJHMT*, Vol. 56, pp. 197 – 205.

Croiset, E., Thambimuthu, K. V., 2001. "NOx and SO_2 emissions from O_2/CO_2 recycle coal combustion". *Fuel*, Vol. 80, pp. 2117-2121.

Di Blasi, C. and Branca, C., 2001. "Kinetics of primary product formation from wood pyrolysis". *Industrial and Engineering Chemistry Research*, vol. 40, p. 5547-5556.

Dorigon, L.J., Duciak, G., Brittes, R., Cassol, F., Galarça, M. and França, F. H. R., 2013. "WSGG correlations based on HITEMP2010 for computation of thermal radiation in non-isothermal, non-homogeneous H_2O/CO_2 mixtures", *Int. Journal of Heat and Mass Transfer*, Vol. 64, pp. 863-873.

Eaton, A.M., Smoot, L.D., Hill, S.C. and Eatough, C.N., 1999. "Components, formulations, solutions, evaluations, and application of comprehensive combustion models". *Progress in Energy and Comb. Sci*., Vol. 25, pp. 387-436.

Filkoski, R.V.; 2010. "Pulverised-Coal Combustion with Staged Air Introduction: CFD Analysis with Different Thermal Radiation Methods". *The Open Thermodynamics Journal*, vol. 4, pp. 2-12,.

Grieco, E. and Baldi, G., 2011. "Analysis and modelling of wood pyrolysis". *Chemical Engineering Science*, v.66, p. 650-660.

Gu, M., Chen, G., Zhang, M., Huang, D.F., Chaubal, P. and Zhou, C.Q., 2010. "Three-Dimensional Simulation of the Pulverized Coal Combustion Inside Blast Furnace Tuyere". *Appl. Math. Modell*, vol. 34, pp. 3536-3546.

Gubba, S.R., Ingham, D.B., Larsen, K.J., Ma, L., Pourkashanian, M., Tan, H. Z., Williams, A. and Zhou, H., 2012. "Numerical modeling of the co-firing of pulverized coal and straw in a 300 MW tangentially fired boiler". *Fuel Processing Technology*, vol. 104, pp. 181–188.

Haseli, Y., Van Oijen, J. A. and De Goey, L. H. P., 2011. "A detailed one-dimensional model of combustion of a woody biomass particle". *Bioresource Technology*, vol. 102, pp. 9772-9782.

Hobbs, M. L., Radulovic, P. T. and Smoot, L. D., 1992. "Modeling fixed-bed coal gasifiers". *AIChE Journal*, Vol. 38, pp. 681-702.

Hottel, H.C. and Sarofim, A.F., 1967. "Radiative Transfer". McGraw-Hill Book Company, New York.

Kuo, K. K., 2005. "Principles of Combustion", John Wiley & Sons, New York.

Liu, H., Zailani, R., Gibbis, B.M., 2005. "Comparisons of pulverized coal combustion in air and in mixtures of O_2/CO_2". *Fuel*, Vol. 84, pp 833 – 840.

Mehrabian, R., Zahirovic, S., Scharler, R., Obernberger, I., Kleditzsch, S., Wirtz, S., Scherer, V., Lu, H. and Baxter, L., 2012. "A CFD model for thermal conversion of thermally thick biomass particles". *Fuel Processing Technology*, vol. 95, pp. 96-108.

Nikuradse, J., 1933. "Strömungsgesetze in rauhen Rohren: aus d. Kaiser-Wilhelm-Inst. f. Strömungsforschg, Göttingen". *In*: Vol. 361 of Forschungsheft, Verein Deutscher Ingenieure, VDI-Verlag Edn., pp. 22.

Patankar, S.V. Numerical Heat Transfer and Fluid Flow. Hemisphere:Washington, DC, 1980.

Rothman, L.S., Gordon, I.E., Barber, R.J., Dothe, H., Gamache, R.R., Goldman, A., Perevalov, V.I., Tashkun, S.A., Tennyson, J., 2010, HITEMP, the high-temperatura molecular spectroscopic database, Journal of Quantitative Spectroscopy and Radiative Transfer, Vol. 111, pp. 2139-2150.

Sami, M., Annamalai, K. and Wooldridge, M., 2001. "Co-firing of coal and biomass fuel blends". *Progress in Energy and Combustion Science*, Vol. 27, pp 171 – 214.

Silva, C.V., Beskow, A.B., Felipetto, L.L., Velicko, A.J., Kominkiewicz, M.J., Pereira, F.M. and Indrusiak, M.L.S., 2015. "CFD analysis of the co-combustion process of coal and woody biomass: particle size influence. *In*: 23rd ABCM International Congress of Mechanical Engineering, December 6-11, Rio de Janeiro, RJ, Brazil

Silva, C. V., Indrusiak, M. L. S. and Beskow, A., 2010."CFD analysis of the pulverized coal combustion processes in a 160 MWe tangentially-fired-boiler of a thermal power plant". *JBSME*, Vol. XXXII, n.4, pp. 328-336.

Turns, S.R., 2000, "An introduction to combustion: concepts and applications", McGraw-Hill.

Ubhayakar, S. W., Stickler, D. B., Rosenberg JR., C. W. and Gannon, R. E., 1976. "Rapid Devolatilization of Pulverized Coal in Hot Combustion Gases". *In*: Symp. Int. on Combustion, The Combustion Institute, Vol. 16, pp. 427-436.

Warnatz, J.; Maas, U.; Dibble, R. W., 1999 "Combustion". Springer: Berlim.

Westbrok, CK.. and Drier, C.K., 1981. "Simplified reaction mechanisms for the oxidation of hydrocarbon fuels in flames". *Combustion Science and Technology*, Vol. 27, pp. 31-46.

Wilcox, D.C.. Reassessment of the scale-determining equation for advenced turbulence models. *AIAA Journal*, Vol. 26, pp. 1299-1310, 1988.

Williams, A., Pourkashanian, M. and Jones, J.M., 2001. "Combustion of pulverized coal and biomass". *Progress in Energy and Combustion Science*, Vol. 27, pp 587 – 610.

Xianchun, L., Hui, S., Qi, W., Chatphol, M., Terry, W. and Jianglong, Y., 2009. "Experimental study on drying and moisture re-adsorption kinetics of an Indonesian low rank coal". *Journal of Environmental Sciences Supplement*, vol. 5, pp. 127-130.

Xu, M., Azevedo, J. L. T. and Carvalho, M. G., 2000. "Modeling of the combustion process and NOx emission in a utility boiler". *Fuel*, vol. 79, pp. 1611-1619.

Yin, C., Kaer, S. K., Rosendahl, L. and Hvid, S.L., 2010. "Co-firing straw with coal in a swirl-stablilized dual-feed burner: modeling and experimental validation". *Bioresource Technology*, vol. 101, pp. 4169-4178.

11. RESPONSIBILITY NOTICE

The authors are the only responsible for the printed material included in this paper.